Available online at www.sciencedirect.com

ScienceDirect

Procedia Manufacturing 47 (2020) 904–909

Procedia MANUFACTURING

www.elsevier.com/locate/procedia

23rd International Conference on Material Forming (ESAFORM 2020)

Study of Tailor Heat Treated Blanks Using the Fourier-series-based VFM

Marco Rossi[a,*], Attilio Lattanzi[a], Antonio Piccininni[b], Pasquale Guglielmi [b], Gianfranco Palumbo[b]

[a]*Dipartimento di Ingegneria Industriale e Scienze Matematiche, Università Politecnica delle Marche, via Brecce Bianche, 60131 Ancona, Italy*
[b]*Department of Mechanical Engineering, Mathematics & Management Engineering, Division of Production Technologies, Polytecnic University of Bari, via Orabona 4, 70125 Bari, Italy*

* Corresponding author. Tel.: +39 071 2204440; fax: +39 071 2204801. *E-mail address:* m.rossi@staff.univpm.it

Abstract

In this work, the Virtual Fields Method (VFM) was used to identify the properties of tailor heat treated (THT) blanks, in terms of different hardening parameters. The spatial variation of the hardening parameters was described using the Fourier series approach. The chosen material is an aluminum alloy 5754 H111 that undergoes a localized heat treatment. From the blank sheet, dog-bone specimens were cut and treated using a laser in the central zone. Tensile tests were performed on the sample using Digital Image Correlation (DIC) to obtain the full-field deformation history. Finally, the F-VFM was applied to identify the spatial distribution of the hardening parameters. In order to compare the results with reference values, further tests were conducted on not treated specimens. Thus, the so-called Fourier-based VFM (F-VFM) was introduced for finite deformation plasticity problems; numerical data are used to validate the inverse approach, and, afterwards, the inverse identification process is applied on experimental data from THT specimens.

Keywords: Inverse identification; Virtual Fields Method; Large deformations; Fourier series; Tailor heat threated blank; Digital Image Correlation

1. Introduction

Tailored blanks are often used in the industry to produce lightweight components with enhanced structural performance. Instead of using tailored blanks with different thickness, localized heat treatments can be used to suitably modify the initial sheet metal blank, in order to optimize the material properties for the following forming operations. This technology is usually named tailor heat treated (THT) blanks [1]. A critical point of this apinproach is the correct evaluation of the heterogenous properties of the THT blanks after the treatment, in order to develop and calibrate appropriate constitutive models for the description of the variable behavior. Recently, the rapid diffusion of full-field measurement techniques like the Digital Image Correlation (DIC) [2] was followed by the development of methods to inversely calibrate complex material models [3]. The use of heterogeneous strain fields, in fact, allows to gather a larger amount of material information from a single test, including the spatial distribution of the stiffness and hardening properties. The Virtual Fields Method (VFM) [4], represents one of the most widespread inverse techniques, and it has been successfully implemented in many non-linear plasticity problems in the case of isotropic [5] and anisotropic behavior [6-8]; Pierron et al. [9] applied the VFM to cyclic plasticity with kinematic hardening, and Fu et al. [10] to the HAH distortional plasticity model.

The VFM was also used to determine the stiffness distribution, this latter expressed by the Fourier transform in the 2-D spatial domain in [11-12]. Cao et al. [13] exploited the concept of the Fourier-series-based Virtual Fields Method (F-VFM) to investigate the elastic modulus distribution of laser repaired GH4169, involving uniaxial tensile tests and full-field measurement data achieved via Moirè Interferometry. In this paper, the concept of F-VFM is extended to non-linear finite deformation plasticity problems, in order to determine the

10.1016/j.promfg.2020.04.278

spatial distribution of the hardening parameters of tailored heat treated specimens of aluminum alloy 5754.

2. The Fourier-based Virtual Fields Method for non-linear material models

The VFM is an inverse method based on the Principle of Virtual Work and allows to identify the material coefficients of a given constitutive model from full-field kinematic data and loading. In the finite deformation plasticity framework, the VFM is expressed by using the Lagrangian description through the following cost function:

$$\Psi(\boldsymbol{\xi}) = \sum_{i=1}^{N_{vf}} \sum_{j=1}^{N_{step}} \left| \int_V \mathbf{T}_j^{1PK} : \delta \mathbf{F}_i^{\bullet} \, dv - \int_{\partial V} \left(\mathbf{T}_j^{1PK} \mathbf{n} \right) \cdot \delta \mathbf{u}_i \, dS \right| \quad (1)$$

where $\mathbf{T}_j^{1PK}$ is the 1st Piola-Kirchhoff stress tensor, $\delta \mathbf{u}_i$ is a virtual displacement field kinematically admissible with the problem, $\delta \mathbf{F}_i^{\bullet}$ is the corresponding virtual displacement gradient tensor, V is the volume of the inspected solid, ∂V is the boundary surface and $\mathbf{n}$ the surface normal. In particular, the first integral represents the Internal Virtual Work, where the stress tensor is calculated from the measured full-field strain data according to constitutive parameters $\boldsymbol{\xi}$; on the other hand, the second integral indicates the External Virtual Work, which is calculated considering the loading force measured during the test. The cost function is evaluated for all the N_{step} timesteps recorded during the test and for all N_{vf} virtual fields introduced. Since the constitutive behaviour is described by a non-linear relationship, the identification is achieved through the minimization of the cost function $\Psi(\boldsymbol{\xi})$ by means of an optimization algorithm.

The selection of the virtual fields is a crucial step for the definition of the VFM cost function, since they weight and activate the information contained by each material point, affecting the accuracy of the identification results. Basically, two main approaches are usually adopted according to the method used for their generation: with the first one, the virtual fields are manually defined by the user, generally employing polynomial or harmonic functions; the second approach automatically creates the virtual fields following some predefined generation criteria. For example, these criteria are based on the minimization of the noise effects on the identification results [9]; in [14], the virtual fields are generated according to the sensitivity of the stress field to each constitutive parameter. Considering this latter method, when a single material parameter ξ_i is perturbed, it is possible to highlight the material points where ξ_i effectively influences the stress calculation. Thereby, the stress sensitivity maps are obtained as:

$$\delta \mathbf{T}_i^{1PK}(\boldsymbol{\xi}, t) = \mathbf{T}^{1PK}(\boldsymbol{\xi} - \delta \xi_i, t) - \mathbf{T}^{1PK}(\boldsymbol{\xi}, t) \quad (2)$$

where, the $\delta \xi_i$ indicates the perturbation of parameter ξ_i, here assumed equal to 0.2. Such stress sensitivity maps are, then, used to build the virtual fields by means of piecewise functions. In other words, the domain is subdivided in a virtual mesh of 4-nodes quadrilateral elements, and a set of virtual nodal displacements, whose gradient produces virtual strain fields similar to the stress sensitivity maps, is defined. For further details the reader is referred to [14].

According to [11], the Fourier series can be exploited to describe the spatial distribution of the material properties. Basically, a general constitutive parameter ξ_i which shows a variable behaviour according to the coordinates of the material point, can be expressed through the combination of harmonic functions in the spatial domain *(x,y)*:

$$\xi_i(x,y) = \sum_{m=0}^{M} \sum_{n=-N}^{N} a_{m,n} \cos\left[2\pi \left(\frac{mx}{L_x} + \frac{ny}{L_y} \right) \right] + \sum_{m=0}^{M} \sum_{n=-N}^{N} b_{m,n} \sin\left[2\pi \left(\frac{mx}{L_x} + \frac{ny}{L_y} \right) \right] \quad (3)$$

where $a_{m,n}$ and $b_{m,n}$ are the coefficients of the Fourier transforms with spatial frequency components (m,n), M and N represents the maximum order of the Fourier series, L_x and L_y are the dimensions of the domain. In this way, the constitutive parameters are described by the Fourier coefficients, which became the objective of the minimization process. This also means that the order of the Fourier series is defined *a priori* at the beginning of the non-linear VFM identification.

3. Experiments on THT specimens

The effects produced by the tailor heat treatment were investigated experimentally performing tensile tests on standard uniaxial specimens with gauge length L_s=70 mm and width w_s=20 mm. The samples were obtained from an aluminum alloy 5754 H111 blank sheet 1.5 mm thick, at 0° with respect to the rolling direction (RD). In the central part of the specimen, a localized zone 10 mm wide was treated by using a laser to heat up to 450°C the zone for 2 s.

Tensile tests were carried out employing an electromechanical testing machine (Zwick-Roell® Z050) at strain rate of 10^{-4} s^{-1}. The loading force was measured with a load cell of 50 kN, and the strain field was measured by using DIC in order to capture strain heterogeneity during the deformation process. In particular, a 3D-DIC setup composed by two CMOS cameras (Pixelink BU371F), with spatial resolution of 1280×1024 pixels, was used, while the full-field displacement measurement was achieved by using the commercial software MatchID® (www.matchid.eu). In all the analysis, the image correlation was performed following the local DIC approach, imposing a subset size of 21 pixels and a stepsize of 7 pixels.

In order to analyze the effects induced by the THT, the gauge area of the specimen is divided into 12 regions of interest (ROI), as depicted in Fig. 1.

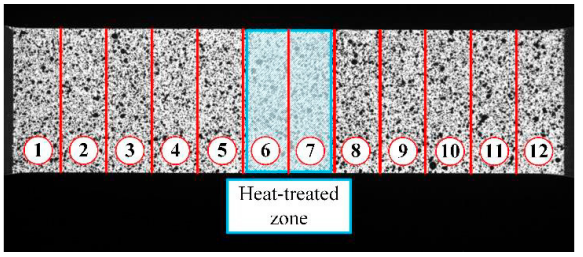

Fig. 1. ROIs located on the specimen surface. The heat-treated zone is indicated in the centre of the specimen.

Thus, the strain fields measured from each ROI is exploited to calculate the corresponding stress-strain curves up to the specimen failure. Fig. 2 reports the comparison of the logarithmic stress-strain curves obtained.

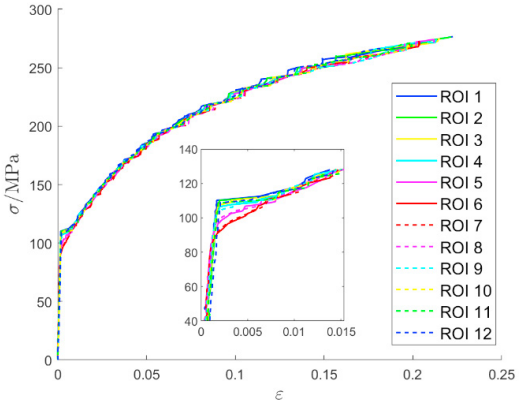

Fig. 2. Logarithmic σ-ε curves measured on the 12 different ROIs.

Considering the elastic behavior, the THT process does not produces modification on the distribution of the elastic stiffness. Nonetheless, the first yielding changes according to the horizontal coordinate of the specimen. In fact, ROI 6 and ROI 7, which correspond to the heat-threated zone, show a lower initial yielding point with respect to the ROI 1 and ROI 12. It is also worth noting that the heat treatment modifies the material behavior for the first values accumulated plastic strains, eliminating the plateau displayed by the untreated zone up to ε=0.01. Moreover, the THT effect is not limited only to the specimen area directly hit by the laser; in fact, ROI 5 and ROI 8 present a transitional behavior due to the heat diffusion during the treatment.

When the plastic work increases, the spatial heterogeneity of the hardening behavior tends to disappear, and the Portevin-Le Chatelier effect (PLC) [15] becomes predominant, producing the typical fluctuations on the σ-ε curves. This is observed also by looking at the strain field measured on the specimen surface (Fig.3), where the bands of strain localization related to the PLC are clearly visible.

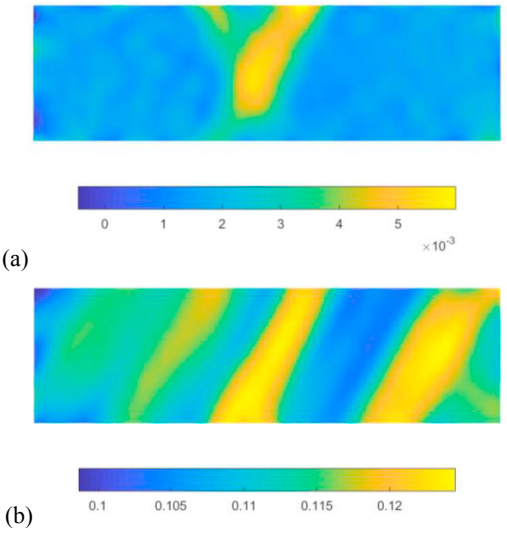

Fig. 3. Measured heterogeneous strain field ε_{xx} (logarithmic), related to the PLC effect: (a) initial stage of plastic deformation; (b) fully developed plasticity.

The outcomes from the analysis on different ROIs are compared with the reference stress-strain curves obtained from the tensile test on untreated specimens (Fig. 4). For the sake of clarity, in this comparison only the stress-strain curves obtained from ROI 1 and ROI 6 are considered. As expected, ROI 1 has the same behavior of the untreated H111 state, while ROI 6 differs in the initial yielding zone.

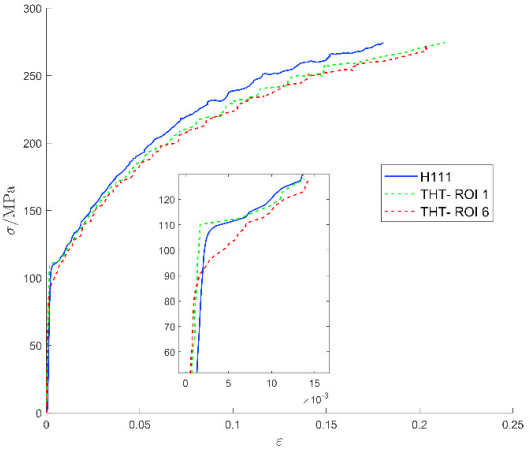

Fig. 4. Comparison of the logarithmic σ-ε curves with AA5457 H32 and H111 reference curves.

3. Numerical validation of the Fourier-based VFM for non-linear problems

The validation of the inverse identification approach described in this paper was firstly performed on numerical data. Therefore, a FE model of the uniaxial tensile test was built by using the implicit code Abaqus\Standard, where the material

model was implemented through a UMAT subroutine. Isotropic Von Mises plasticity was assumed, and the hardening behavior was described by the Voce hardening law:

$$\bar{\sigma} = A_H - B_H \cdot \exp(-C_H \bar{\varepsilon}_P) \tag{4}$$

where $\bar{\sigma}$ indicates the yield stress, A_H B_H C_H are the parameters of the hardening model, and $\bar{\varepsilon}_P$ represents the accumulated equivalent plastic strain according to the principle of plastic work equivalence. The spatial distribution of the hardening behavior was modelled expressing the constitutive parameter B_H through the Fourier series and considering that B_H changes only with the horizontal coordinate x. Thereby, Eq. 3 is rewritten as:

$$\bar{\sigma} = A_H - B_H(x) \cdot \exp(-C_H \bar{\varepsilon}_P) \tag{5}$$

where:

$$B_H(x) = \sum_{m=0}^{M} a_m \cos\left[2\pi\left(\frac{mx}{L_x}\right)\right] + \sum_{m=1}^{M} b_m \sin\left[2\pi\left(\frac{mx}{L_x}\right)\right] \tag{6}$$

Fig. 5 illustrates the FE model mesh and the applied boundary conditions. Four-nodes plane stress elements (CPS4) with full-integration were adopted to discretize the geometry. A total displacement of 2.5 mm was imposed on the right side of the specimen, while the horizontal displacement of the left side was blocked.

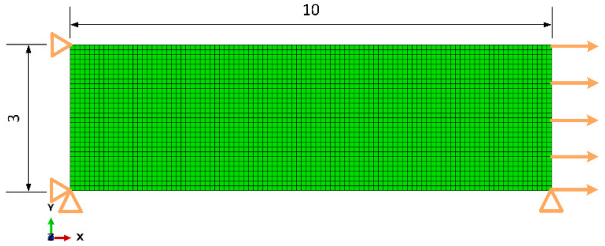

Fig. 5. FE model adopted for the validation of the F-VFM.

The reference material parameters for the FE model were chosen in order to reproduce a general 5xxx series aluminum alloy, and they are all listed in Tab. 1. Fig. 6 reports the two different hardening curves introduced to model the untreated and thermally treated zones.

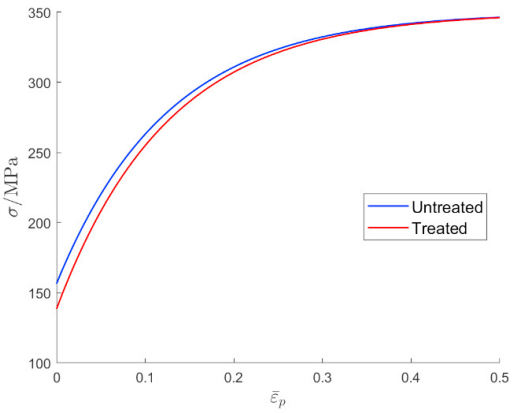

Fig. 6. Hardening behavior for the treated and untreated zones of the specimen.

In this analysis, the spatial distribution of the parameter $B_H(x)$ was described involving Fourier series with order M=2; this leads to the introduction of 6 Fourier coefficients in the VFM cost function. It also worth noting that the two coefficients b_1 and b_2 are imposed equal to zero in order to exclude sinusoidal terms from Eq. 6. This assumption makes the distribution of the heterogenous hardening properties similar to the one observed experimentally in Section 2, where the maximum change of material properties is localized in the central part of the specimen (Fig. 7).

Table 1. Reference material parameters of the FE model

Elastic Properties:	
E	70 GPa
ν	0.3
Voce hardening law coefficients:	
A_H	350
C_H	8
$B_H(x)$ Fourier coefficients:	
a_0	200
a_1	-9
a_2	2.5
b_1	0
b_2	0

The non-linear VFM identification was conducted on 25 timesteps, and the virtual fields were automatically generated exploiting the stress sensitivity related to each constitutive parameter. The cost function minimization was addressed to the identification of only the three Fourier series coefficients a_0, a_1, a_2; this allows to constrain the optimization algorithm to focus on the coefficients regulating the spatial distribution of the constitutive parameter, giving a more precise insight of the non-linear VFM behavior coupled with Fourier series. The minimization process was accomplished by the Levenberg-Marquardt algorithm (LMA), using, as stopping criteria, a threshold of 10^{-9} for the cost function and a tolerance of 10^{-10} on the minimum parameters change. The identification outcomes are listed in Tab. 2.

Table 2. Identified Fourier coefficients on numerical data.

a_0	a_1	a_2
203.3424	-9.4524	2.5173

Fig. 7 compares the spatial distribution of $B_H(x)$ provided by the identified parameters with the reference one introduced in the FE model, showing a good agreement between the two sets of data, with a maximum error of 1.6%.

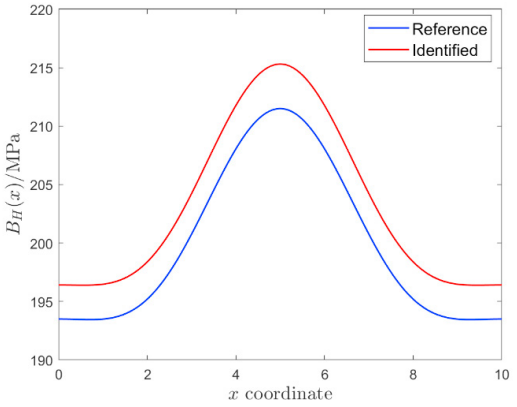

Fig. 7. Spatial distribution of the parameter $B_H(x)$ according to the identified Fourier coefficients on numerical data.

4. Identification of the spatial distribution of the hardening behavior for THT blanks

The inverse identification framework based on the non-linear VFM and the Fourier series was used to characterize the spatial variation of the hardening parameters for the AA5754, whose properties were locally altered through THT. Thus, the measured strain fields from the uniaxial tensile test were adopted to feed the VFM identification procedure, adopting the same approach reported for the numerical validation. Therefore, the experimental data from the reference AA5754 H32 (not thermally treated) were used to model the global plastic behavior of the material by means of the Voce hardening law (Fig. 8). As before, the spatial variation of the hardening behavior was handled by expressing the material parameter $B_H(x)$ through a Fourier series and keeping the A_H and C_H coefficients constant. The Fourier series is considered until the order M=2, and the sinusoidal components were neglected ($b_1 = b_2 = 0$). Such assumption, in fact, helps to mitigate the disturbing effect related to generation and movement of Portevin-Le Chatelier bands during the deformation process. All the input material coefficients not involved in the identification process are reported in Tab. 3, where the coefficient $B_H^{[H32]}$ is the one resulting from the Voce fitting on the untreated H111 experimental data and is used as initial guess for the coefficient a_0.

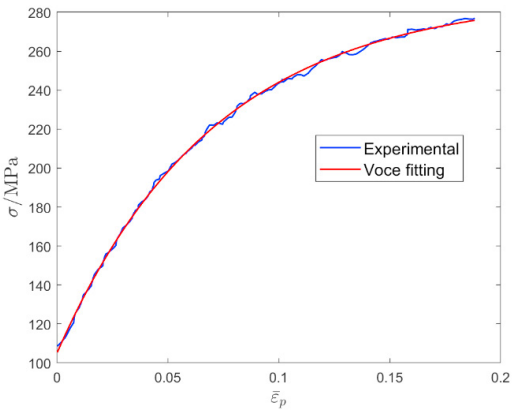

Fig. 8. Voce hardening law fitting with AA5754 H111 experimental data.

Table 3. AA5754 THT material coefficients not submitted to VFM identification.

Elastic Properties:	
E	70 GPa
ν	0.3
Voce hardening law coefficients:	
A_H	288.6
$B_H^{[H32]}$	183.9
C_H	14.17

The non-linear VFM cost function minimization was performed on 30 steps equally spaced along the time history of the test, involving three sets of virtual fields based on the stress sensitivity according to Eq. 2. Tab. 4 summarizes the identified Fourier coefficients. The accuracy of the identification results is evaluated comparing the flow stress curves calculated from the VFM outcomes with the ones retrieved experimentally in the treated and untreated zones (Fig. 9). Although the spatial dependency was accounted only to a single material parameter, the corresponding identified Fourier coefficients are capable of reproducing the drop of the first yielding point produced by the heat treatment. Nonetheless, there is a bias between the inversely calibrated curves with the experiments for higher values of equivalent plastic strain; this difference, however, is related to the initial calibration of the Voce law coefficients A_H and C_H on the untreated AA5754 H32 data, which, also, display a similar shift with respect to treated specimen in Fig. 4.

Table 4. Identified Fourier coefficients on experimental data.

a_0	a_1	a_2
194.8674	7.6942	-0.4712

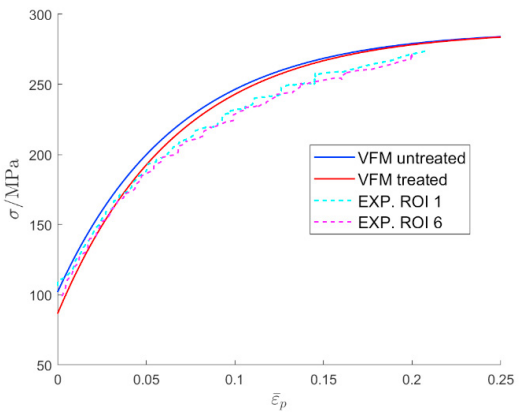

Fig. 9. Comparison between identified and experimental flow stress curves in two different zones.

Fig. 10 depicts the resulting spatial distribution of the parameter B_H, highlighting the highest difference in correspondence of the zone directly hit by the laser for the heating treatment.

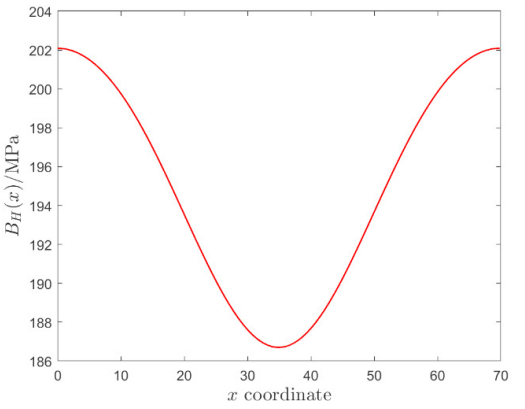

Fig. 10. Spatial distribution of the material parameter $B_H(x)$ according to the identified Fourier coefficients on experimental data.

5. Conclusions

In this paper, the non-linear VFM is used to identify the spatial distribution of THT blanks of AA5754, in terms of different hardening parameters. The spatial variation of the hardening parameters was described using the Fourier approach. Experimental tests were performed on uniaxial tensile specimens, where the central part of the gauge region was thermally treated for 2 s at the temperature of 450°C. The displacement and strain field measured by using DIC are used to investigate the effects induced by the THT. In particular, the heat treatment mainly alters the hardening behavior of the initial stages of the plastic deformation, changing the first yielding point.

The full-field data are also employed to perform an inverse identification with the non-linear VFM. First, the non-linear VFM coupled with the Fourier Transforms was validated on numerical data, and then applied to the experiments. The identified parameters are in agreement with the reference hardening behavior measured on the treated and untreated zones of the THT specimen. In future, more aspects concerning the order of the Fourier series, the impacts of the Portevin-Le Chatelier effect on the spatial distribution of the hardening behavior will be investigated in detail.

References

[1] Geiger M, Merklein M, Vogt U. Aluminum tailored heat treated blanks. Prod Eng Res Devel 2009; 3:401.
[2] Sutton MA, Orteu JJ, Schreier HW. Image correlation for shape, motion and deformation measurements. Springer; 2009.
[3] Avril S, Bonnet M, Bretelle A-S, Grédiac M, Hild F, Ienny F, Latourte F, Lemosse D, Pagano P, Pagnacco E, Pierron F. Overview of identication methods of mechanical properties based on full-eld measurements. Exp Mech 2008; 48:381-402.
[4] Pierron F, Gréediac M. The Virtual Fields Method. Springer; 2012.
[5] Gréediac M, Pierron F. Applying the Virtual Fields Method to the identication of elasto-plastic constitutive parameters. Int J Plasticity 2006; 22:602-627.
[6] Rossi M, Pierron F. Identication of plastic constitutive parameters at large deformations from three dimensional displacement fields. Comp Mech 2012; 49:53-71.
[7] Lattanzi A, Barlat F, Pierron F, Marek A, Rossi M. Inverse indentification strategies for the characterization of transformation-based anisotropic plasticity models with the non-linear VFM. Int J Mech Sci 2020; 105422.
[8] Rossi M, Pierron F, Stamborska M. Application of the Virtual Fields Method to large strain anisotropic plasticity. Int J Solids Struct 2016; 97-98:322-335.
[9] Pierron F, Avril S, The Tran V. Extension of the Virtual Fields Method to elasto-plastic material identification with cyclic loads and kinematic hardening. Int J Solids Struct 2010; 47:2993-3010.
[10] Fu J, Barlat F, Kim J-H. Parameter identifcation of the homogeneous anisotropic hardening model using the Virtual Fields Method. Int J of Mater Form 2015; 9(5):691-696
[11] Nguyen TT, Huntley JM, Ashcroft IA, Ruiz PD, Pierron F. A Fourier-series-based Virtual Fields Method for the identification of 2-D stiffness distributions. Int J Numer Meth Eng 2014; 98:917-936.
[12] Nguyen TT, Huntley JM, Ashcroft IA, Ruiz PD, Pierron F. A Fourier-series-based Virtual Fields Method for the identification of 2-D stiffness and traction distributions. Strain 2014; 50:454-468.
[13] Cao QK, Xie HM, Wang H. Fourier-series-based virtual fields method combining with Moirè interferometry for characterising elastic modulus distribution of laser repaired GH4169. Strain 2018; 55:e12299.
[14] Marek A, Davis FM, Rossi M, Pierron F. Extension of the sensitivity-based virtual fields to large deformation anisotropic plasticity. Int J Mater Form 2019; 12(3):457-476.
[15] Kang J, Wilkinson D, Jain M, Embury J, Beaudoin A, Kim S, Mishira R, Sachdev A. On the sequence of inhomogeneous deformation processes occurring during tensile deformation of strip cast AA5754, Acta Mater 2006; 54: 209-218.